

Visualization of Surface and Subsurface Morphology: The Effect of Processing on a Rubber-Modified Thermoplastic

S. A. Edwards, N. Roy Choudhury, M. Provas

Polymer Science Sector, Ian Wark Research Institute, University of South Australia, Mawson Lakes Boulevard, Mawson Lakes, SA 5095, Australia

Received 6 July 2001; accepted 27 April 2002

ABSTRACT: In typical injection-molding processes, variation in the quality of the surface finish is often encountered. To understand the mechanism of common surface defect formation, we investigated the effect of processing parameters on the morphological features of a commercially supplied polycarbonate/acrylonitrile–styrene–acrylate rubber-modified thermoplastic blend. A compositional analysis of the material was performed with thermogravimetric analysis. Acid and alkaline etching, in conjunction with scanning electron microscopy, was used to characterize the effect of various injection times, packing pressures, and material tem-

peratures on the morphology of processed parts. Chemical etching revealed that the injection molding had a large influence on the morphology of the thermoplastic, particularly on the surface, where preferential phase segregation produced a highly oriented polycarbonate skin layer. The degree of molecular orientation on the surfaces of molded parts had a significant effect on the efficiency of both the acid- and alkaline-etching techniques. © 2002 Wiley Periodicals, Inc. *J Appl Polym Sci* 87: 774–786, 2003

Key words: injection molding; morphology; polycarbonates

INTRODUCTION

Injection molding is a process in which a molten plastic is forced into a cold mold in which it is cooled and solidified to form a specific product.¹ Because polymers are poor thermal conductors, there is a large temperature gradient present when the gate freezes. The interior material continues to cool and shrink, but the material that has already frozen opposes this shrinkage. This produces thermoelastic stresses in the interior of the plastic and may result in part failure. These stress and thermal shrinkage phenomena will often cause product distortion and result in a marred visual appearance. Defects that occur on the outer surface of the molded part pose a problem because they lower the surface quality of the finished product. In any complex manufacturing process, the key to minimizing such problems is to completely understand the process, materials, and equipment involved.

Previous studies² on the effect of injection-molding parameters on the properties of molded parts have demonstrated that there are five main controllable factors. These include the injection time, material temperature, mold temperature, pack pressure, and cavity pressure, all of which play significant roles during the injection cycle to various degrees. High mold temper-

atures are known to improve surface appearance significantly. Molten plastic, at elevated temperatures, has a lower viscosity and, therefore, a better flow behavior, thereby reducing shear stress. With the injection time increased, the shear stress also increases, and this results in flow instabilities and, therefore, a poor surface finish.

Over the past several years, there has been a considerable amount of work devoted to understanding the effects of the packing pressure phase, yielding data that recognize this parameter as the single most dominant cause of the various properties in injection-molded parts.^{3,4} The higher the packing pressure is, the higher the yield modulus and the ultimate tensile strength become. This is due to more efficient packing of the material. Additionally, higher molecular orientation is often the result of an increase in pack pressure.

To adequately characterize the effect of injection-molding parameters on the surface finish, we must fully describe that material's multiphase morphology. In typical multiphase thermoplastics, such as acrylonitrile–butadiene–styrene (ABS) or acrylonitrile–styrene–acrylate (ASA), a minor portion of rubber (5–20%) is incorporated as a dispersed phase into a rigid plastic matrix. For improved coupling to the styrene–acrylonitrile (SAN) continuous phase, the rubber phase is grafted with the same monomeric building blocks of which the resin phase consists.⁵ Therefore, the final product will consist of both bound and unbound rubber phases.

Correspondence to: N. Roy Choudhury (namita.choudhury@unisa.edu.au).

Contract grant sponsor: Australian Research Council.

In typical rubber-modified plastics, the size and distribution of rubber particles contained within the matrix may determine such properties as the impact strength, surface finish, and processability. In particular, the particle size can pose a conflicting dilemma during processing, especially when the product is used in an outdoor automotive application for which cosmetic appeal is of paramount importance. The smaller the rubber particle is, the better the surface finish is. This is due to the enhancement of relaxation and recovery effects that take place in the melt during solidification. Smaller particles can pose a problem, however, as they are inefficient and ineffective in initiating and terminating crazes, respectively, thereby increasing the rates of creep.⁵ The incorporation of larger particles will enhance a material's impact strength but will produce the opposite effect on the quality of the surface finish, creating the need for a particle size compromise.

The relationship between the amount of rubber and the surface finish of injection-molded parts has been well documented in the literature.⁶ Materials with decreasing rubber levels will increase the recoverable shear strain, yet decrease the shear stress. These two factors have the combined effect of improving the overall surface finish.

Blends of polycarbonate (PC) and ABS have been used commercially for some time. Recently, a trend has developed of traditional ABS being replaced with ASA. ASA has properties similar to those of ABS, with the added advantage of enhanced thermal properties due to the replacement of polybutadiene (containing a susceptible double bond) with a polyacrylate. Little published research on ASA exists, despite its potential as a rigid toughened material.⁷

In a heterogeneous polymer blend, the microscale morphology is a major determinant of many bulk and surface properties. Although there has been a considerable amount of work investigating the various types of morphologies prevalent within thermoplastics and their blends,⁷⁻⁹ there is a distinct lack of documentation linking this characteristic to processing and surface finish. Traditionally, morphology has been studied through the scanning electron microscopy (SEM) of fractured surfaces and transmission electron microscopy. These methods, although successful, are often hindered because of a lack of contrast between phases.¹⁰ Chemical etching by alkaline and acid solutions can provide a good method for complementary morphology observations of polymeric blends.¹¹

The physiochemical approach to morphology determination involves selectively removing one phase through the etching of the polymer surface and subsequently examining its topography. A solution of chromic acid will oxidize the rubber particles within a thermoplastic such as ABS or ASA and leave the SAN matrix untouched.¹² Alternatively, an analysis of PC

blends can be achieved through the use of a strong alkaline solution of either sodium or potassium hydroxide. This basic solution succeeds in selectively hydrolyzing PC on blend surfaces.¹⁰ Resulting SEM images will visually supply knowledge of phase orientation due to the molding cycle, establishing a processing fingerprint.

Although etching techniques for morphological investigations have been available for some time and are relatively simple to perform, little attention has been devoted to their applications to rubber-modified blends of PC and ABS or ASA in the literature. Both acid- and alkaline-etching techniques, developed by Bucknall et al.¹¹ and Eastmond and Smith,¹⁰ respectively, have been used in characterizing the morphology of self-prepared thermoplastic blends.¹² Few studies have investigated the effect of injection molding on the quality of commercially available blends. Hamada and Tsunasawa¹³ successfully used the oxidation of polybutadiene to correlate the formation of flow marks to the internal structure of a commercial structure of a commercial PC/ABS blend. Their results suggested that flow marks were deposited on the surfaces of parts because of a disruption in the tip of the PC flow front that caused PC and ABS to coexist at the surface.

The aim of this study was to gain in-depth insight into the nature of the morphology generated as a result of flow during processing. The morphology of a commercially supplied PC/ASA sample used in the injection molding of automotive applications was investigated. The general composition analysis of the material was performed with thermogravimetric analysis (TGA), a technique that accurately measures weight changes with temperature. Chemical etching, in conjunction with SEM, was used to characterize the effect of various injection times, packing pressures, and material temperatures on the morphology of processed parts. A better understanding of the effect of the processing conditions on the morphological features of these thermoplastics can yield insight into the mechanism of surface defect formation.

EXPERIMENTAL

Materials

Geloy XP4025 PC/ASA was received from GE Plastics, SA, Australia. Raw, pelleted material was injection-molded into plaques (285 mm × 75 mm × 3 mm) with a Ludwig Engel model ES 700/150 injection-molding machine (Maschinefabrik, Schwertberg, Austria) coupled with a mild steel plaque tool. Table I lists the injection-molding processing conditions that were used to produce defected plaques. A total of 15 plaques per condition were manufactured with these settings. An initial purge period was used to dispose

TABLE I
Injection-Molding Parameters for Engineered Plaques

Plaque no.	Condition summary	Injection time (s)	Pack pressure (bar)	Material temperature (°C)
1	Ideal	2.6	55	260
2	PPH, MTH, ITF	1.1	75	275
3	PPL, MTL, ITF	1.2	15	245
4	PPH, MTH, ITS	6.9	100	275
5	PPL, MTL, ITS	7.0	15	245

PPH: pack pressure high; MTH: material temperature high; PPL: park pressure low; MTL: material temperature low; ITS: injection time slow; ITF: injection time fast.

of any material remaining from the previous runs. For convenience, the analysis of unprocessed PC/ASA was performed on compression-molded samples produced in an electrically heated press at 240°C with a plaque mold.

Compositional analysis: TGA

TGA of pelleted Gelyo PC/ASA was conducted with a TGA 2950 thermal analyzer (TA Instruments) with a conventional (heating rate) mode. Conventional thermogravimetry (TG) was operated from 200 to 800°C at a heating rate of 10°C/min for an evaluation of the blend composition. TG experiments were carried out in duplicate, first under a nitrogen atmosphere until 500°C and then by a burn in oxygen, both at a flow rate of 60 mL/min. In all experiments, a nominal, 15-mg sample was used.

Etching procedure

Chemical etching was performed with both chromic acid (method A) and aqueous NaOH (method B) solutions.

Method A

Chromic acid was prepared by the addition of 5 g of sodium dichromate ($\text{Na}_2\text{Cr}_2\text{O}_7$) to 5 mL of water and 95 mL of concentrated sulfuric acid with constant stirring. No further dilutions were necessary as the original solution proved adequate in contrasting the blend's multiphase morphology. The acidic solution was applied to compression-molded sheets at various etching times of 0.5, 1, 5, and 15 min, washed in water, and oven-dried at 80°C for 1 h for an evaluation of the rubber particle size and distribution in the unprocessed state. Injection-molded plaques were similarly etched for 0.5, 2, and 5 min but at different cross-sectional (perpendicular to flow) and defected (dull edge) locations along the sample.

Method B

Both compression-molded sheets and ideally injection-molded plaques were exposed to a reflux system of aqueous NaOH (30% w/v) at a constant temperature of 105°C over etching times of 0.5, 1, 1.5, and 6 h. After the controlled etch, samples were washed thoroughly in warm water and oven-dried at 80°C for 1 h.

Morphology observations: SEM

All chemically etched specimens were coated with carbon/gold and analyzed under a Phillips XL20 scanning electron microscope (TA Instruments, New Castle, DE) with an accelerating voltage of 10 kV and a spot size of 4.

RESULTS AND DISCUSSION

Surface finish

All plaques, even those molded under ideal conditions, display a variety of surface defects. Plaque 1 shows the best overall surface finish but is flawed around the edges, with a variation in the gloss that appears as a dull line. A sink mark is also evident in the center of the part and is due to the position of the ejector pins on the other side of the mold. Plaques 2 and 4, molded at higher packing pressures and material temperatures but at different injection speeds, display a finish similar to what is seen in the ideal part. However, both parts display stress marks around the gate, and that plaque produced at a higher injection speed displays flash along one edge. Plaque 3, produced at a low pack pressure, a low material temperature, and a fast injection time, also shows an overall finish similar to the ideal. Various surface defects can be seen, however, including surface ring marks and tiger stripe stress marks along the upper edge of the part. Finally, plaque 5, produced as a short shot because of the mild processing conditions used during its production, reveals ring marks and dimpled edges. The direct morphological analysis of defects is limited to the edge defects during this work. Further study,

TABLE II
Composition Analysis by TGA

Transition	Temperature at peak maximum (°C)	Weight loss (%)	Component
1	405.3	80.3	SAN and Poly butyl acrylate
2	471.3	10.6	PC
3	540.7 (under O ₂)	9.1	Filler

however, concentrated on the direct analysis of other such defects (described) is underway and will be published later.

Determination of composition by TGA

Tabulated data from the weight-loss and derivative weight-loss curves for unprocessed PC/ASA are shown in Table II. TGA clearly shows three weight-loss transitions corresponding to ASA, PC, and the burning of filler in oxygen. SAN and polybutylacrylate degraded in the same temperature range corresponding to a weight loss of 80.3% at 405°C. PC degrades at a higher temperature of 471°C and is detected in lower quantities at 10.6%. Remaining fillers, which included stabilizers and carbon black, were burnt in oxygen and made up 9.1% of the total composition. These results confirm that this blend consists of an ASA matrix containing a low content of PC.

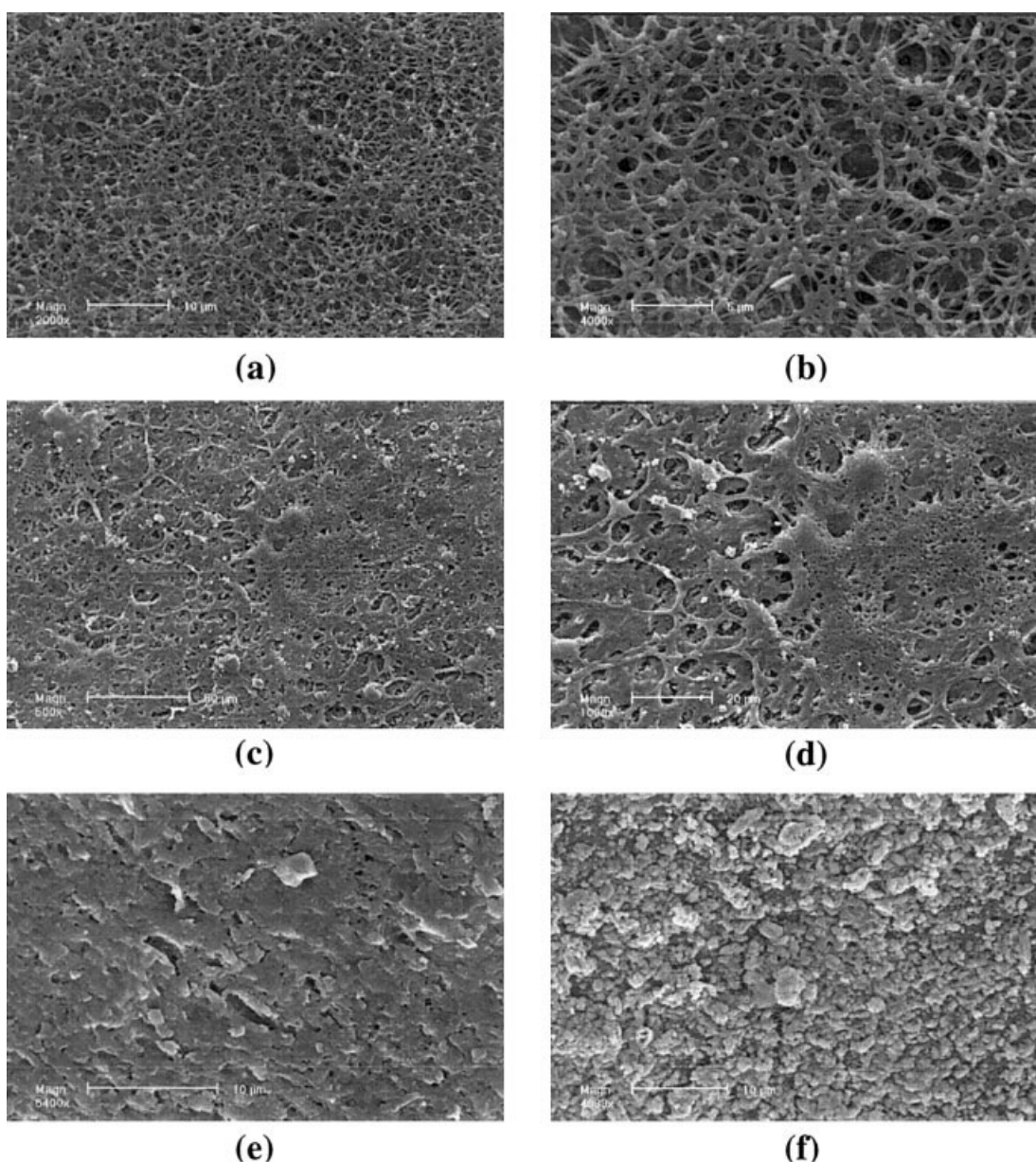


Figure 1 SEM images of compression-molded PC/ASA etched with chromic acid for (a,b) 30 s, (c,d) 1 min, (e) 5 min, and (f) 15 min.

TABLE III
Cavity Size and Distribution for Both Unprocessed and Processed PC/ASA

Sample (etch time)	Average cavity size (μm)	Cavity surface population (cavities/ mm^2 of surface)
Compression molded PC/ASA (30 s)	0.3–2.6 (average 1.2 ± 0.6)	N/A
Plaque 1 (5 min)	70×49	31
Plaque 2 (5 min)	108×62	45
Plaque 3 (5 min)	108×57	36
Plaque 4 (5 min)	73×48	62
Plaque 5 (5 min)	67×37	28

N/A = not applicable.

Visualization of surface and subsurface morphology by acid etching: compression molding versus injection molding

Figure 1 displays the SEM images of compression-molded PC/ASA etched with chromic acid at various times. In these micrographs, the dark areas are the voids left by the extracted rubber. Etching with chromic acid at 30 s [Fig. 1(a,b), different magnifications] has selectively removed the polybutylacrylate rubber phase, leaving a rough surface with numerous ex-rubber cavities and enabling the visualization of the rubber particle size and distribution. A closer view of this sample surface reveals some knotlike features. These images effectively contrast the morphology of PC/ASA. Chemical attack has revealed two general sizes of cavities (Table III) within an etching-resistant micronetwork pertaining to both SAN and PC. The variations in the cavity size are consistent with the structural model for rubber-modified thermoplastics, indicating both bound and unbound particles. No evidence of particle orientation can be seen on the surface; this suggests that compression molding applies little stress to the material, which is, therefore, a good representation of raw, unprocessed material. In addition, at high magnification [Fig. 1(b)], small nodes can be seen that may indicate the process of phase opening. As rubber is extracted from the surface and subsurface regions, both SAN and PC will yield, curling and forming weblike structures.

SEM of samples etched for 1 min [Fig. 1(c,d)] displays images with a clear morphological contrast and two general sizes of ex-rubber cavities. The progress of etching is notably more advanced, evidenced by the amount of surface rubble that can be seen at high magnifications. Two regions of varying etching patterns are displayed. One region contains holes of two general sizes, and another has only one, indicating that the unprocessed plastic, even after compression molding, shows signs of incomplete phase mixing and nonhomogeneous flow. It is thought that the zone with a single hole size is PC and that the region with two sizes is SAN, displaying both bound and unbound properties.

The severity of over-exposure to chromic acid attack can be clearly noticed from the morphological features at etching times of 5 and 15 min [Fig. 1(e,f)]. Phase contrast at this stage is impossible, as the surface has disintegrated and has been reduced to a debris field of etching-resistant and oxidized particles.

Identical physiochemical attack by chromic acid was applied to ideally processed injection-molded plaques to gauge the effect of processing on the PC/ASA blend. SEM images of plaque 1, similarly etched at times of 0.5, 2, and 5 min, are displayed in Figure 2. From the outset, it is clear that the morphological design of the surface differs from that of the unprocessed material because little evidence of rubber oxidation is visible at an etching time of 30 s [Fig. 2(a)]. The surface has remained very smooth, and it is not until 2 min of etching time that the true surface-phase variation between processed and unprocessed materials becomes apparent.

Figure 2(b,c) shows the resulting SEM of plaque 1 etched at 2 min. These surfaces are different from those of Figure 1. Large, oval-shaped cavities are seen, at even low magnifications, distributed across the entire surface. The hole size and depth are many times larger than that seen in the unprocessed material, and all are similarly oriented and elongated to the direction of flow. At first glance, it appears that a surface rubber agglomeration mechanism exists during processing. This, however, would still leave regions on the surface that mimic those images seen in Figure 1(a–d). On closer inspection, the surface contains large swellings that appear to be early-stage cavities that have not emerged at this etching time. This reveals that etching is occurring as a result of the slow diffusion of chromic acid to the subsurface, demonstrating that the surface is constructed of a chromic acid-resistant PC phase. Those cavities are thought to be the result of a PC phase opening and subsequent subsurface etching, with the dissolved rubber phase exploding through the surface. Additionally, lips seen around holes [see Fig. 2(c,e,f)] indicate phase opening, again pointing to etching at subsurface depths. This visually confirms our earlier work¹⁴ by microthermal

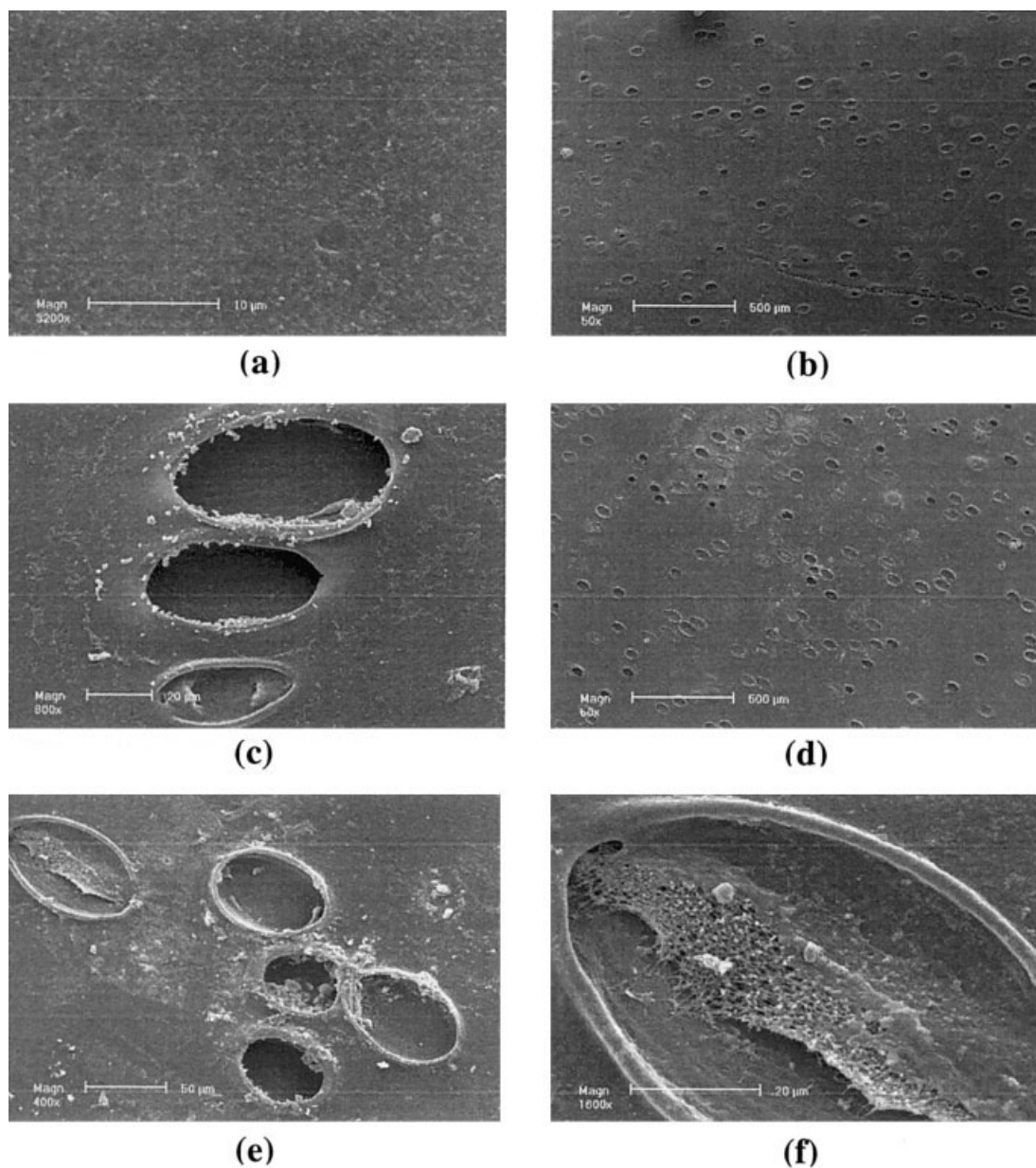


Figure 2 SEM images of an ideally injection-molded PC/ASA (plaque 1) etched with chromic acid for (a,b) 30 s, (b,c) 2 min, and (d,f) 5 min.

analysis (μ TATM), which suggested that preferential phase segregation during injection molding causes a dominant PC skin layer on the surfaces of parts. This phenomenon is due to each material's flow and viscosity characteristics, which promote preferential phase segregation. In the blend, PC is the lower molecular weight component and, therefore, flows well and forms the skin layer for those parts produced with a glossy finish. Separate studies on the flow marks and internal structure of PC/ABS blends¹³ have drawn similar conclusions.

It must also be mentioned that the phase morphology of a blend system changes as a function of its composition, the intrinsic viscosity of the components,

the shear rate, the temperature of processing, and so forth. Moreover, the morphology is dependent on the thermodynamic properties of the components during processing. The viscosity of each component¹⁵ during processing generally determines and/or dictates which phase is continuous. However, it is quite evident that systems with greater differences in component melt viscosities show larger cavities (compression vs injection).

Etching for 5 min reveals a similar micrograph image. Longer exposure to chromic acid has produced numerous, larger holes that are again oriented to the direction of flow. Such an appearance on the surface suggests that a morphological change has occurred in

the sample after processing, simply by a coarsening mechanism. Such coarsening occurs as a result of melt agglomeration in such systems in which rubber particles are not considerably crosslinked. Crosslinking of the particles can greatly improve the quality of the part as it offers a route to control the particle size by preventing agglomeration. Studies seeking information on the degree of rubber crosslinking in this system with solvent extraction and pyrolysis are currently underway.

Longer exposure times also reveal fewer swellings or ghost holes as well as a greater presence of rubble, which indicates advanced etching. On closer analysis at higher magnifications, a different type of morphology is seen within the basins of some cavities [Fig. 2(f)]. This region resembles an unprocessed state, signifying that the morphology at the subsurface to bulk regions may reflect rawlike structures. Cross-sectional etching studies were undertaken to investigate this phenomenon and are also discussed in this article.

Effect of processing conditions on surface and subsurface morphology by acid etching

The quality of any injection-molded product is greatly affected by the gate location. Overall gate design is an important factor in molding because it influences the style in which the plastic flows into the mold cavity. In this study, all parts have been injection-molded with an end-gated plaque tool. This causes a variance in the melt flow between positions both near and far from the gate. The resulting flow pattern from an end-gated system results in a part with less directionally balanced morphological properties. In this work, all test specimens have been sampled from the center of the plaque, unless otherwise indicated.

Those plaques produced at extreme injection-molding conditions have also been exposed to chromic acid to evaluate the effect of processing on their surface and subsurface morphologies. Figure 3 displays the SEM images obtained by etching at 2 and 5 min for both plaques 2 and 3. Images for plaque 2, molded at a faster injection time, a higher pack pressure, and a higher material temperature, show a morphology similar to that seen in the ideal part. At longer etching times, however, there is an increase in the hole size and number. The average hole size (Table III) has increased from $70\ \mu\text{m} \times 49\ \mu\text{m}$ (plaque 1) to $108\ \mu\text{m} \times 62\ \mu\text{m}$. Both effects are hypothesized to be caused by greater packing due to higher pressures and temperatures resulting in better melt flow and mold filling.

Plaque 3 displays a comparable number of cavities in comparison with plaque 1. The hole size has once again risen to an average dimension of $108\ \mu\text{m} \times 57\ \mu\text{m}$. This is due to an elongation mechanism seen on many of the holes [Fig. 3(f–h)], most noticeably at

5-min etching times. It is theorized that a combination of fast injection times and lower packing pressures and temperatures results in a low-viscosity melt and highly forced injection through the nozzle, promoting high shear and elongation flows at the mold wall. These forces would result in the stretched, oval-shaped holes seen readily on plaque 3. Both plaques 2 and 3 have the largest cavity dimensions of all the molded parts.

A closer analysis by SEM on plaques produced at slower injection times shows variations in the morphology seen at fast injection times. Figure 4 displays the images obtained for both plaques 4 and 5. At first glance, cavities on both plaques appear smaller. Plaque 4 [Fig. 4(a–d)], molded at a high pack pressure and material temperature, has an average cavity size of $73\ \mu\text{m} \times 48\ \mu\text{m}$. Comparably, plaque 5 [Fig. 4(e–h)], molded at a low pack pressure and material temperature, had a similar average cavity size of $67\ \mu\text{m} \times 37\ \mu\text{m}$. Slower injection times, regardless of pack pressure and material temperature levels, promote longer cycle times and result in smaller cavity dimensions.

Variations in the number of cavities per unit area (determined from a 5-min etching time), detailed in Table III, reveal unique and contrasting information for each plaque's morphology. Those plaques, molded at high pack pressure and material temperature, show the greatest cavity surface population, particularly at slow injection times. Lower cavity populations are seen on those plaques manufactured at ideal and low-pressure and low-temperature conditions. This knowledge provides an insight into the thickness of the skin layer under various processing conditions. At this stage, it is believed that the cavity size does not represent the morphology of the rubber particles but rather represents the result of a PC skin opening. The morphological aspect of the rubber component becomes visible inside the cavities.

Investigation of cross-sectional morphology by acid etching

To understand the skin/core morphology in detail for the injection-molded samples, we have used microtoming so that a given section of a plaque represents the overall morphological texture. To gauge the thickness of the formed PC layer and its morphological effects within the subsurface to bulk regions, plaque 1 was cross-sectioned, perpendicular to the direction of flow, and exposed to chromic acid for 2 min. Three distinct regions of various phase morphologies are evident and are displayed in Figure 5. Figure 5(a) clearly shows the plaque surface and a region, 30–40 μm thick, in which no etching has occurred. This acid-resistant zone is the PC layer and is consistent across the entire length of the part to a similar depth.

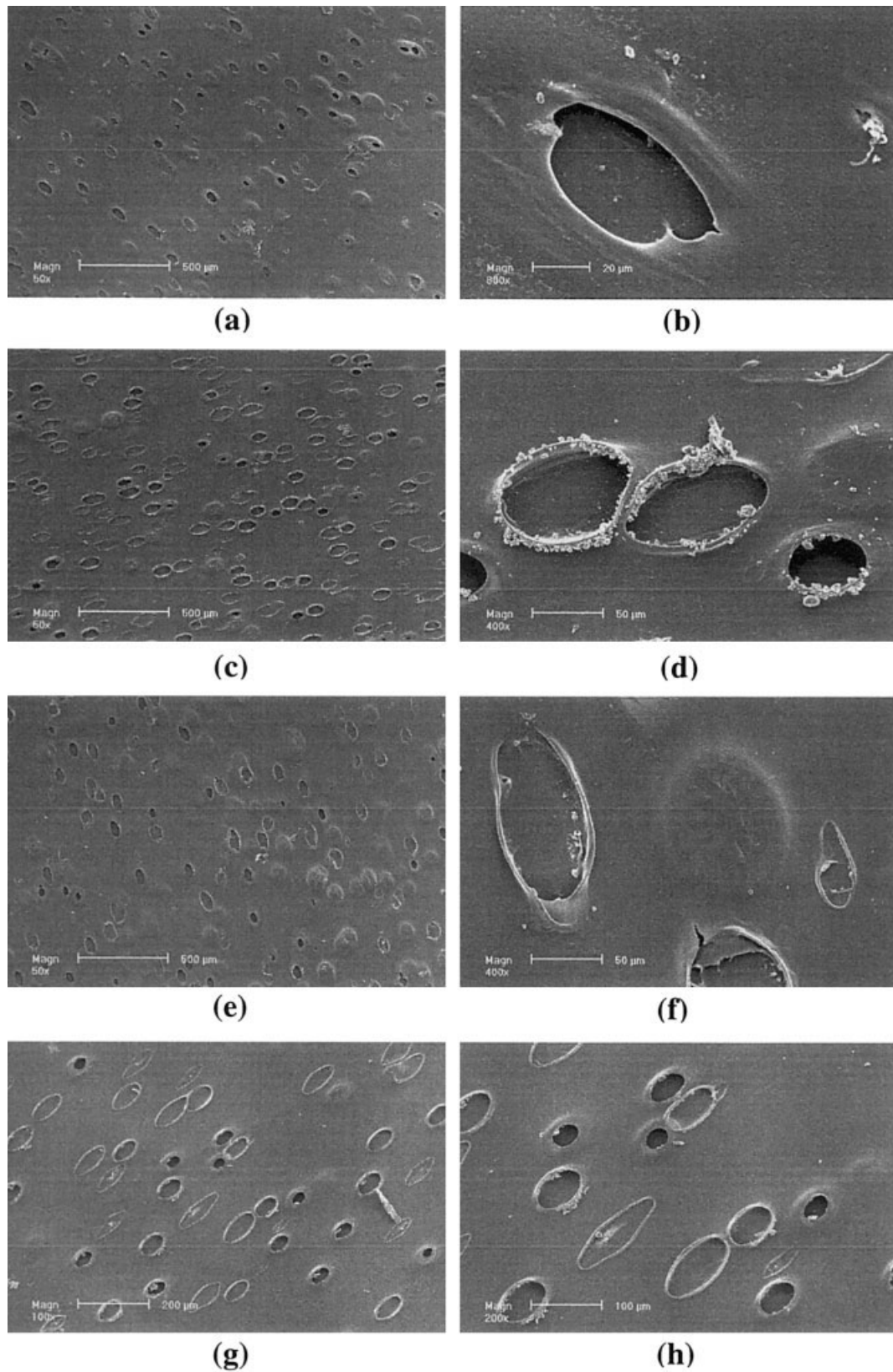


Figure 3 SEM images of chromic acid-etched plaques injection-molded with short injection times at both high and low pack pressures and material temperatures: plaque 2, etched for (a,b) 2 and (c,d) 5 min, and plaque 3, etched for (e,f) 2 and (g,h) 5 min.

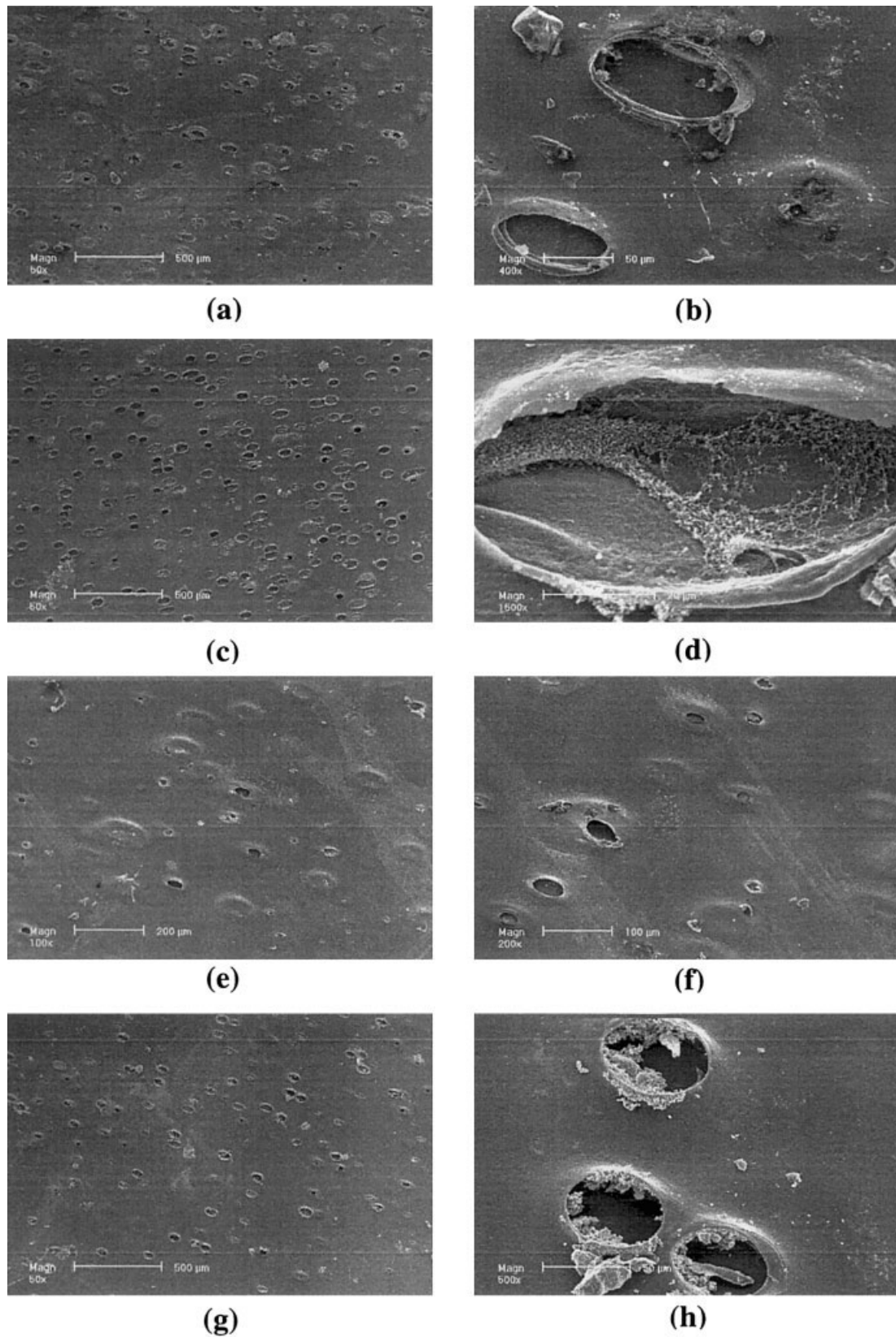


Figure 4 SEM images of chromic acid-etched plaques injection-molded with long injection times at both high and low pack pressures and material temperatures: plaque 4, etched for (a,b) 2 and (c,d) 5 min, and plaque 5, etched for (e,f) 2 and (g,h) 5 min.

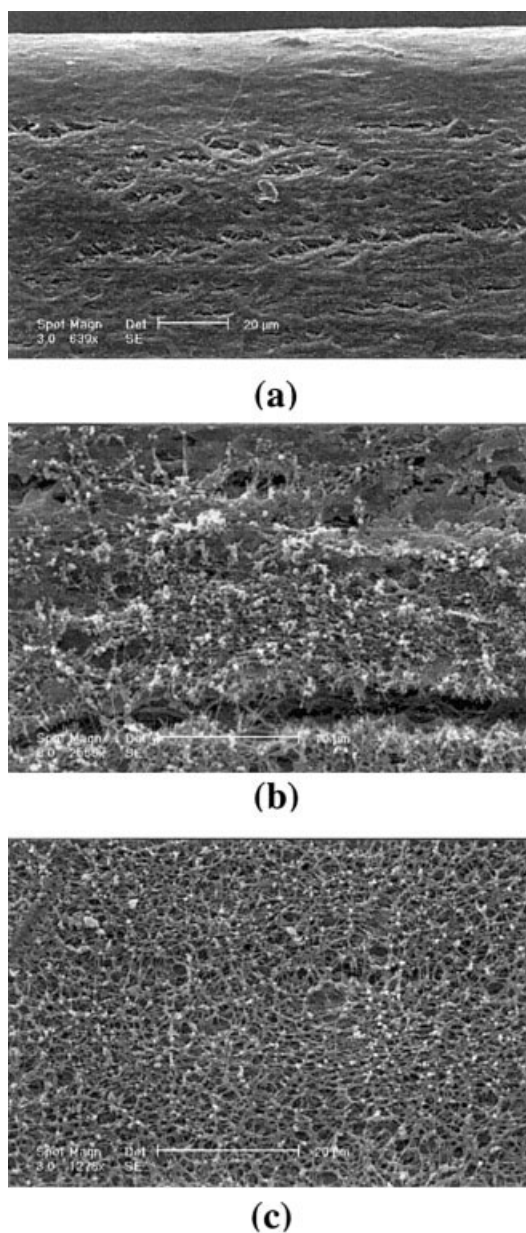


Figure 5 SEM images of cross-sectioned specimens of plaque 1 etched with chromic acid for 2 min.

Intermediate distances from the surface PC phase show a unique morphology [Fig. 5(b)]. It can be described as containing a combination of both an etching-resistant phase, as seen in Figure 5(a), and an etched unprocessed zone of a fibrillate nature, as shown earlier in Figure 1(a,b). This suggests that there is a PC/ASA phase gradient extending into the bulk, consisting of a PC-rich skin layer, followed by an intermediate layer, with the amount of ASA increasing toward the subsurface zones. Our earlier studies¹⁴ with localized thermal analysis made similar conclusions with depth-profiling techniques using μ TATM.

It is clear that there is a decrease in the molecular orientation in the core, with the bulk region [Fig. 5(c)]

showing a morphology identical to that seen previously in unprocessed PC/ASA. The rubber particle size and overall distribution are again evident. This indicates that any morphological effects resulting from the many forces applied during injection molding are more apparent on the surface and subsurface layers of PC/ASA blends, rather than in the bulk. These observations are predominantly caused by variations of the shear rate within the mold, between the melt at the wall and part core. The melt flow within the bulk of the mold experiences minimal levels of shear, whereas at the wall, higher levels of the shear rate are seen. At a very high shear rate, wall slippage can occur in which true replication of the mold surface is not possible. This phenomenon, known as stick-slip behavior, results in various types of surface defects, depending on the in situ developed morphology in that region. In general, such velocity profiles result in a skin layer more highly oriented in comparison with the core. Work is currently underway characterizing the interface between ASA and PC at surface and subsurface levels with modulated differential scanning calorimetry to fully understand the morphological effect of injection molding on thermoplastic blends.

Analysis of edge defects by acid etching

The production of a dull finish along the edge of injection-molded plaques proved to be the most consistent and reproducible surface defect during this study. Acid etching was used to investigate the possible link between the morphology and the surface finish along the edges of these parts. Once more, key locations were exposed to chromic acid etching along the edge of plaque 2, which was chosen as the representative plaque because it was produced under the most extreme conditions. Etch locations are detailed in Figure 6, covering edges opposite the gate and near the flash. Resulting SEM images are displayed in Figure 7.

After 5 min of exposure to acid conditions, the usual cavitation and swelling landscape are seen, although there are obvious differences in both locations when the edge of the part is approached. In the two positions, both opposite to the gate and near the flashing

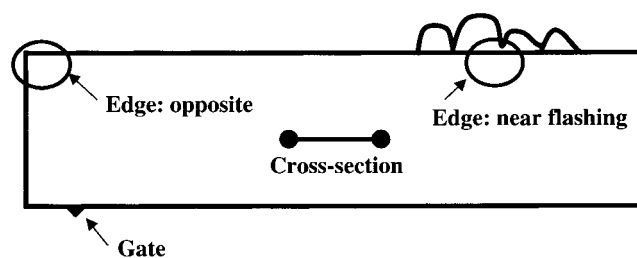


Figure 6 Location of sites on plaque 2 exposed to chromic acid and analyzed by SEM.

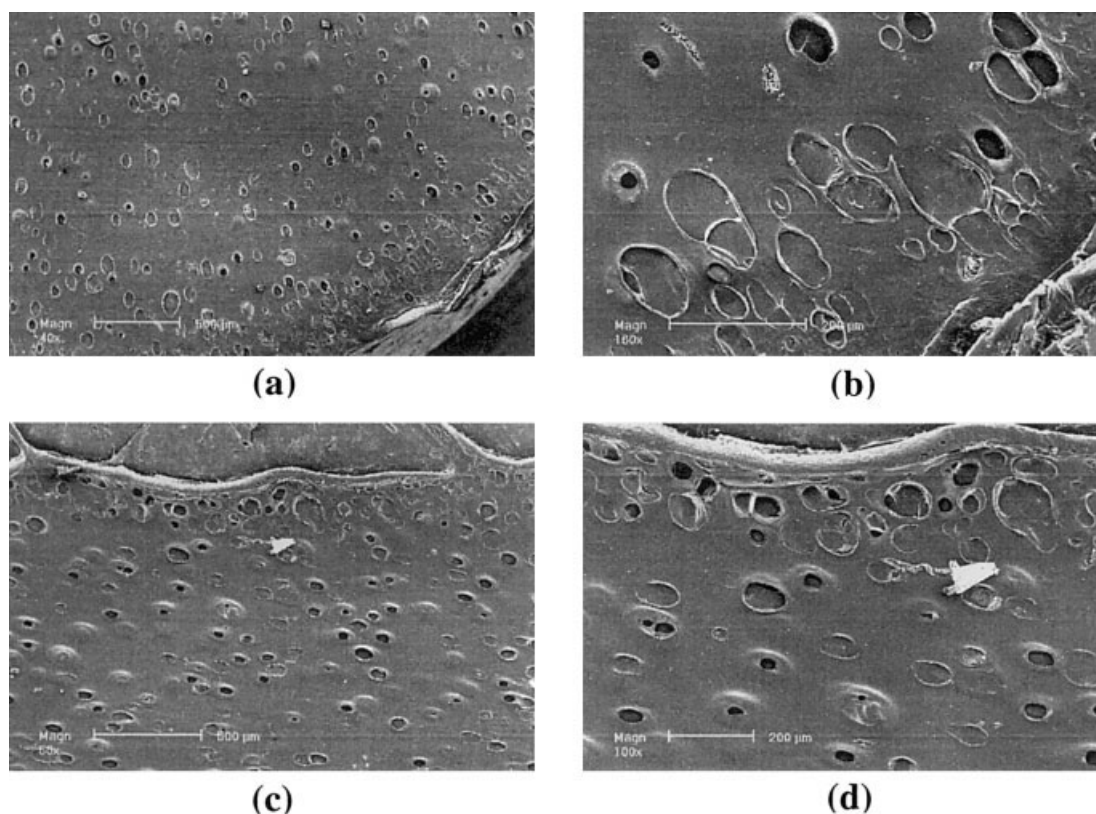


Figure 7 SEM images of locations on plaque 2, at edges both (a,b) near and (c,d) far from the gate, etched with chromic acid for 5 min.

area, the size and number of cavities increase dramatically. These cavities now range in size up to $200\ \mu\text{m}$ in diameter, with a depth far greater than that seen in earlier examples. In Figure 7(c), there are a large number of holes and an even greater number of subsurface swellings. These observations suggest that although a PC phase persists on the surface, there is a greater amount of ASA at the subsurface levels in comparison with the center of the parts.

A comparison of the net cavity orientation both opposite to the gate and near the flash reveals the various flow properties that exist along a part that is end-gated. Opposite the gate, cavity orientation is toward the edge, whereas near the flash, it is parallel to the edge. This pertains to at least two flow directions present along the length of the plaque. Another important observation to note is the varying shape of the cavities at both locations. Close to the gate, cavities are oval-shaped, whereas near the flash region, holes have become more spherical in nature. Near the gate, shear effects at the mold wall are more severe. Additionally, it is generally known that a temperature gradient will exist across a mold, with higher temperatures being found close to the gate because of the proximity of the heated barrel, plastic melt, and high shear at the gate. Therefore, a warmer mold will promote slower cooling times within the melt, resulting in a higher recov-

ery. In combination, as the time to cool is increased in regions close to the gate, stretching and elongation flows will form as the time to the material's no-flow is extended. As the skin layer is frozen to the mold wall, these effects are frozen-in as the material's surface morphology. In cooler regions of the mold away from the gate, elongation mechanisms are still prevalent at the melt-mold interface, although they are minimized as the skin layer is solidified at faster rates. This effect is clearly demonstrated in Figure 7, in which two contrasting morphologies can be seen on two sections of the same part.

Visualization of surface and subsurface morphology by alkaline etching

SEM images of compression-molded PC/ASA, etched with 30% w/v NaOH at 105°C for various times, can be seen in Figure 8. This refluxing alkaline solution hydrolyzes surface PC but leaves the SAN and acrylate rubber components unaffected. Immediately after the application of the base, any surface gloss that is present on the sample is lost, an unremarkable and dull finish being left. This may signify the hydrolyzation of a thin layer of PC, which is responsible for gloss effects. After etching, the alkaline solution possesses a light yellow color in comparison with the

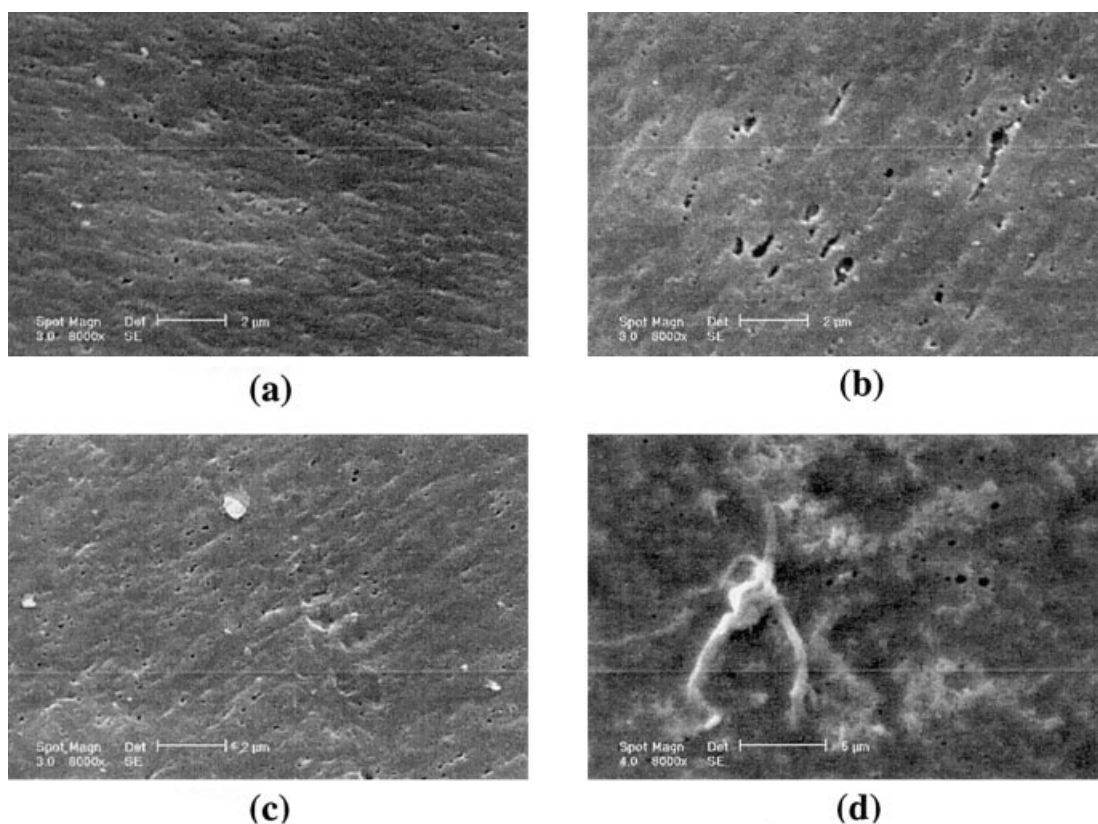


Figure 8 SEM images of compression-molded PC/ASA etched with refluxing 30% (w/v) NaOH for (a) 30 min, (b) 60 min, (c) 90 min, and (d) 6 h.

initial clear solution, indicating that chemical attack has occurred. The resulting surface morphology after etching at 30, 60, and 90 min [Fig. 8(a–c)] appears very similar, indicating that a significant portion of the etching process is completed at low treatment times. The surface is very resistant to caustic attack because of the large quantity of the ASA matrix phase, with small holes and crevices seen where the low-content surface PC, at local structure variation, is contained. This is consistent with earlier results by TGA, which has been used to determine that the thermoplastic consists of 80.3% ASA and 10.6% PC. A similar observation was made by Eastmond and Smith¹⁰ while etching a pure PC film with a similar alkaline solution. Frank et al.¹⁶ also observed a similar structure with an ion-etching technique.

Similarly, those plaques injection-molded under ideal conditions have also been etched via the same alkaline solution. Figure 9 displays the resulting SEM images of plaque 1, which has been alkaline-etched at both 30 and 60 min. As with the compression-molded specimens, a reduction in the surface gloss is noted almost immediately after the application of the base. However, no noticeable color change in the etching solution occurs after exposure to the plastic specimens, and this indicates that a reduced amount of chemical attack may have occurred. Etching at 30 min

[Fig. 9(a,b)] does not reveal the same sporadic, submicrometer cavity landscape as the compression-molded samples do. Rather, elongated and similarly oriented crevices are visible, measuring up to 50 μm long. Etching at 60 min [Fig. 9(c,d)] again shows elongated crevices with matched orientation, although not as obvious as those seen at shorter etching times. However, a longer etching time has produced a number of deeper, smaller cavities that range in size from 10 μm to the submicrometer level.

It is clear that the surface of the plaque is being affected by the application of the base, which can be detected to a certain degree through observations by both direct visual analysis and electron microscopy. However, the amount of chemical attack does not suggest the presence of a dominant PC phase, deposited by a preferential phase-segregation mechanism proposed by both acid etching and μ TATM.¹⁴ This phenomenon may be attributed to the molding process itself, which produces a dense surface morphology vastly different from that of the bulk. The diffusion of the alkaline solution through the skin surface and into the bulk phase will be hindered by the density of the highly oriented and networked skin layer that forms during injection molding, thereby reducing the amount of visible surface etching.

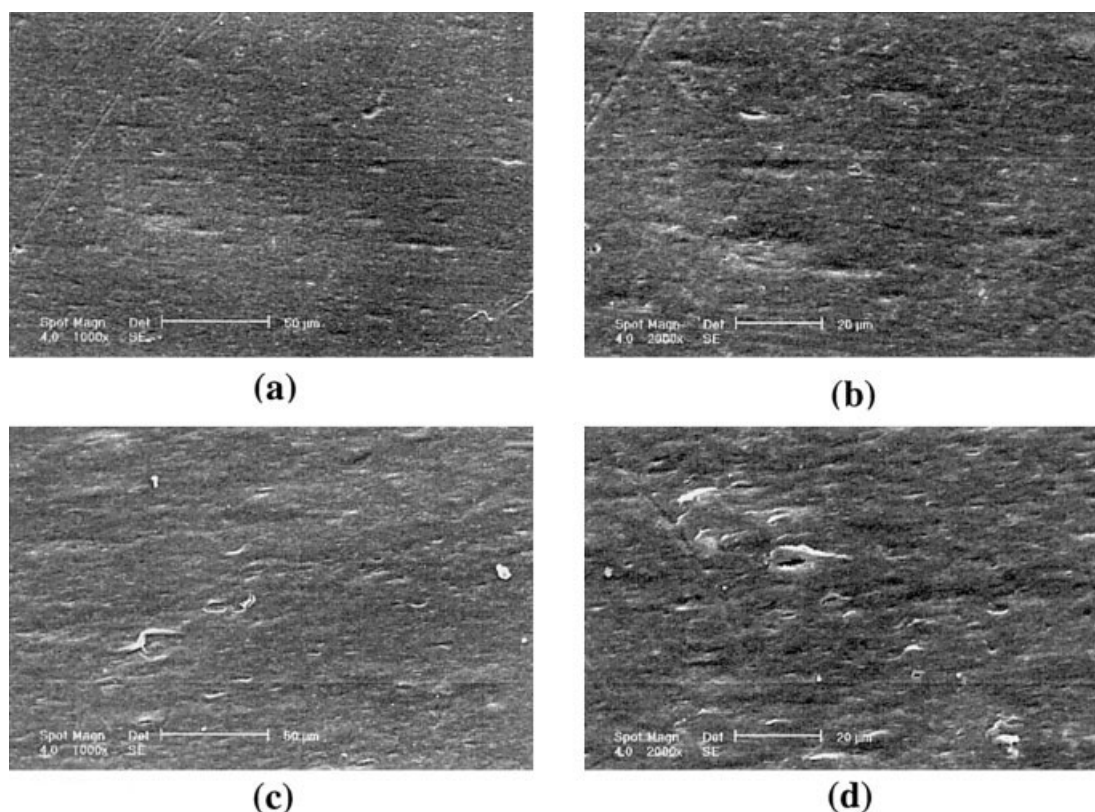


Figure 9 SEM images of an ideally injection-molded PC/ASA (plaque 1) etched with refluxing 30% (w/v) NaOH for (a,b) 30 and (c,d) 60 min.

CONCLUSIONS

Etching by chromic acid and, to a lesser extent, by NaOH is a useful and informative means of contrasting and quantifying the various surface and subsurface morphologies of a PC/ASA blended part, both near and far from the edges or gate. From this study, it is clear that the process of injection molding has a large influence on the morphology of the thermoplastic, particularly at the surface, on which a preferential phase segregation produces a highly oriented PC skin layer. The glossy PC-rich skin layer is followed by an intermediate layer, with the amount of ASA increasing toward the bulk, in which a lower level of molecular orientation exists. An analysis of dull regions close to the plaque edge shows variations in the surface morphology pertaining to the presence of larger quantities of ASA in comparison with glossy regions.

The degree of molecular orientation at the surface has a significant effect on the efficiency of both the acid- and alkaline-etching techniques. The highly oriented skin network that is present in injection-molded parts is difficult to penetrate. This is particularly seen when injection-molded parts are etched with NaOH,

which produces images showing sporadic attack because of variations in the local structure of PC.

References

1. Kennedy, P. *Flow Analysis of Injection Molds*; Hanser: Munich, 1995.
2. Campbell, G. A.; Devanathan, H.; Settlemire, S.; Sweeney, P.; Klewicki, K.; Kenny, T.; Smael, J. D.; Fricke, A. L. *Proc Annu Tech Conf* 1989, 47, 312.
3. Skourlis, T. P.; Mohapatra, C.; Manochchri, C. S. *Adv Polym Sci* 1997, 16, 117.
4. Bushko, W. C.; Stokes, V. K. *Polym Eng Sci* 1995, 35, 365.
5. Bucknall, C. B. *Toughened Plastics*; Applied Science: London, 1977.
6. Chang, M. C. O. *Proc Annu Tech Conf* 1994, 52, 312.
7. Benson, C. M.; Burford, R. P. *J Mater Sci* 1995, 30, 573.
8. Benson, C. M.; Burford, R. P. *J Mater Sci* 1996, 31, 1425.
9. Wildes, G.; Keskkula, H.; Paul, D. R. *Polymer* 1999, 40, 7089.
10. Eastmond, G. C.; Smith, E. G. *Polymer* 1973, 14, 509.
11. Bucknall, C. B.; Drinkwater, I. C.; Keast, W. E. *Polymer* 1973, 13, 115.
12. Dong, L.; Greco, R.; Orsello, G. *Polymer* 1993, 34, 1375.
13. Hamada, H.; Tsunasawa, H. *J Appl Polym Sci* 1996, 60, 353.
14. Provatas, M.; Edwards, S. A.; Roy Choudhury, N. *Thermochim Acta* 2002, 392–393, 339.
15. Kresge, E. N. *J Appl Polym Sci* 1984, 39, 37.
16. Frank, W.; Godder, H.; Stuart, H. A. *J Polym Sci Part B: Polym Lett* 1967, 5, 711.